

Picosecond Dynamics of a Small Molecule in Its Bound State with an Intrinsically Disordered Protein

Gabriella T. Heller, Vaibhav Kumar Shukla, Angelo Miguel Figueiredo, and D. Flemming Hansen*



Cite This: <https://doi.org/10.1021/jacs.3c11614>



Read Online

ACCESS |



Metrics & More



Article Recommendations



Supporting Information

ABSTRACT: Intrinsically disordered proteins (IDPs) are highly dynamic biomolecules that rapidly interconvert among many structural conformations. These dynamic biomolecules are involved in cancers, neurodegeneration, cardiovascular illnesses, and viral infections. Despite their enormous therapeutic potential, IDPs have generally been considered undruggable because of their lack of classical long-lived binding pockets for small molecules. Currently, only a few instances are known where small molecules have been observed to interact with IDPs, and this situation is further exacerbated by the limited sensitivity of experimental techniques to detect such binding events. Here, using experimental nuclear magnetic resonance (NMR) spectroscopy ^{19}F transverse spin-relaxation measurements, we discovered that a small molecule, 5-fluoroindole, interacts with the disordered domains of non-structural protein 5A from hepatitis C virus with a K_d of $260 \pm 110 \mu\text{M}$. Our analysis also allowed us to determine the rotational correlation times (τ_c) for the free and bound states of 5-fluoroindole. In the free state, we observed a rotational correlation time of 27.0 ± 1.3 ps, whereas in the bound state, τ_c only increased to 46 ± 10 ps. Our findings imply that it is possible for small molecules to engage with IDPs in exceptionally dynamic ways, in sharp contrast to the rigid binding modes typically exhibited when small molecules bind to well-defined binding pockets within structured proteins.

One-third of human proteins are intrinsically disordered proteins (IDPs) that rapidly interconvert among different structures.^{3–5} Some IDPs have been suggested to interact with small molecules,^{6–12} thus opening up an enormous class of potential drug targets, especially for conditions including cancers, cardiovascular diseases, type II diabetes, and viral infections.¹³ Nevertheless, the biophysical mechanisms that underpin the binding between small molecules and IDPs are largely based on theoretical molecular dynamics (MD) simulations that, in turn, have suggested that these interactions are highly dynamic.^{6,7,9,14–16} Here, we employ experimental ^{19}F -based nuclear magnetic resonance (NMR) spectroscopy to demonstrate that a small molecule remains extremely dynamic in its bound state with an IDP, in striking contrast to how most small molecules bind to structured proteins.

MD simulations have the potential to offer important insights into interactions between IDPs and small molecules; however, these calculations suffer from force field inaccuracies,^{17–19} and the reliability of these computationally expensive simulations is further hindered by long time scales required to reach convergence, especially for dynamic systems like IDPs, which undergo motions on varying time scales.^{18,19} There is also a lack of available experimental techniques suitable for characterizing interactions between IDPs and small molecules. Most of our high-resolution understanding of small-molecule/drug interactions with proteins comes from experimental X-ray crystallography, which allows scientists to resolve the atomistic details of the binding interactions, primarily enthalpic contributions including electrostatics, hydrogen bonding, π - π stacking, and hydrophobic effects. Due to their highly dynamic nature, IDPs are generally not amenable to crystallography, and given the high entropic costs associated

with folding from a disordered state, it is not yet well-understood whether a small molecule could induce a single, stable structure for such experiments.

NMR spectroscopy uniquely provides atomic-resolution insights into biomolecular interactions in physiological environments,^{20–22} without the need to apply large labels nor localize the molecules on a surface—both of which may alter the structural ensemble and thus the behavior of the IDP. Standard NMR experiments, such as ligand-detected chemical shift perturbations, are commonly employed to screen and assess the binding of small molecules to structured proteins.²³ However, chemical shifts report on the local environment of the nuclei in question, which, in turn, are averaged over time and over all the molecules in solution. Given the proposed dynamic nature of the interactions between IDPs and small-molecule ligands,^{6,7,9,15} we rationalized that NMR parameters that report on ligand dynamics and exchange might be more sensitive to detect IDP/small-molecule binding than chemical shifts.¹² To further enhance the sensitivity of the experiment to binding, we employed ^{19}F instead of ^1H as a probe, as ^{19}F has the advantage that there are no background signals in the NMR spectra from buffer components nor protein, and these spectra therefore exclusively report on the small molecule in question.

Received: October 18, 2023

Revised: January 4, 2024

Accepted: January 5, 2024

We chose the disordered domains 2 and 3 from the non-structural protein 5A (NSSA-D2D3) from the hepatitis C virus

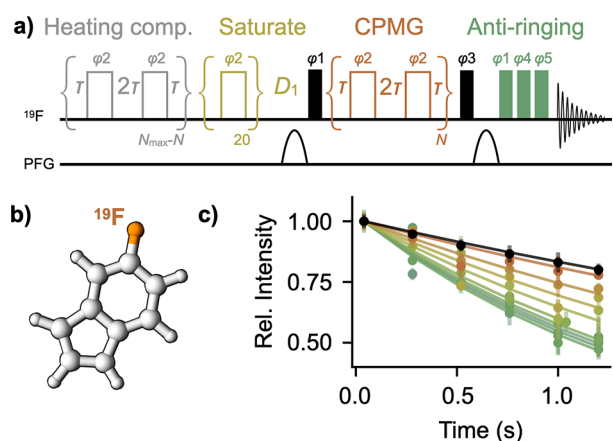


Figure 1. Transverse ^{19}F relaxation ($R_{2,\text{eff}}$) is sensitive to small-molecule binding to a disordered protein. (a) Modified pulse sequence for the ^{19}F $R_{2,\text{eff}}$ experiment.¹ Narrow and wide rectangles indicate 90° and 180° pulses, respectively. The number of CPMG blocks, N , is varied in experiments, while the time of each block, 4τ , is held constant. (b) Structure of 5-fluoroindole. (c) Relaxation curves obtained for $50\ \mu\text{M}$ 5-fluoroindole in the absence and presence of varying concentrations of NSSA-D2D3. Error bars are SEM from ≥ 3 technical replicates.

(JFH-1 genotype) as a model system, given the availability of established purification protocols and chemical shift assignments.^{24–26} Using ^{19}F transverse spin-relaxation rates $R_{2,\text{eff}}$ via a CPMG-based R_2 experiment^{1,27,28} (Figure 1a), we identified that 5-fluoroindole (Figure 1b) interacts with NSSA-D2D3. Specifically, as the concentration of NSSA-D2D3 is increased in samples containing $50\ \mu\text{M}$ 5-fluoroindole, the relaxation curves systematically decrease (Figure 1c), corresponding to an increase in the effective transverse relaxation rate of the ^{19}F spin in 5-fluoroindole, $R_{2,\text{eff}}$ (Figure 2a). Key features of the $R_{2,\text{eff}}$ pulse program (Figure 1a) include 1) a heating compensation element to ensure that the sample is exposed to identical RF power independent of the number of CPMG blocks used¹ and 2) an anti-ringing sequence to remove broad baseline artifacts at the on-resonance ^{19}F frequency that result

from sub-optimal performance of the ^1H RF coil that has been detuned for ^{19}F experiments.^{1,29} We also measured ^{19}F longitudinal relaxation rates $R_{1,\text{eff}}$ (Figure 2b) using an inversion recovery experiment² and ^{19}F chemical shift perturbations (Figure 2c) of $50\ \mu\text{M}$ 5-fluoroindole in the presence of varying concentrations of NSSA-D2D3 and observed systematic changes.

To gain additional insight into the interaction mechanism of 5-fluoroindole with NSSA-D2D3, a simple one-site binding model was assumed, where 5-fluoroindole can exist in one of two states: a “free” form (F) and a “bound” form (B) interacting with NSSA-D2D3. The binding mechanism is likely dynamic and more complex, but here we simply assume the “bound” form represents an ensemble of states all interacting with NSSA-D2D3. The increase in $R_{1,\text{eff}}$ and $R_{2,\text{eff}}$ observed with increasing concentrations of NSSA-D2D3 (Figure 2) could arise from either elevated intrinsic relaxation rates of 5-fluoroindole in the bound conformation or an exchange-induced increase in these relaxation rates.³⁰ To address this, we took an integrative approach: the experimental ^{19}F transverse relaxation, (Figure 2a), ^{19}F longitudinal relaxation (Figure 2b), and ^{19}F chemical shifts (Figure 2c, Figure S1) were combined with translational diffusion measurements of $50\ \mu\text{M}$ 5-fluoroindole, measured by ^1H diffusion ordered spectroscopy (DOSY) (Figure S2). ^1H instead of ^{19}F DOSY measurements were employed due to the relatively increased sensitivity of the ^1H nucleus. ^{19}F transverse relaxation, longitudinal relaxation, and chemical shift data involved titration of NSSA-D2D3 up to $90\ \mu\text{M}$. ^1H DOSY measurements were performed in the absence and presence of $75\ \mu\text{M}$ NSSA-D2D3. All data were analyzed simultaneously within the one-site binding model. In particular, we related free and bound longitudinal and transverse relaxation rates ($R_{1,\text{F}}$, $R_{1,\text{B}}$, $R_{2,\text{F}}$, and $R_{2,\text{B}}$ with free and bound rotational correlation times ($\tau_{\text{c,F}}$ and $\tau_{\text{c,B}}$, respectively) via well-established equations (Supporting Information).^{31–34} The free and bound rotational correlation times, the dissociation rate (k_{off}), the dissociation constant (K_{d}), and the diffusion coefficient of the bound form (D_{B}) were determined from a least-squares analysis; see the Supporting Information. The diffusion coefficient of the free form of 5-fluoroindole (D_{F}) was determined to be $(1.47 \pm 0.02) \times 10^{-9}\ \text{m}^2\ \text{s}^{-1}$ by fitting the ^1H DOSY data in the absence of NSSA-D2D3 (Supporting Information and Figure

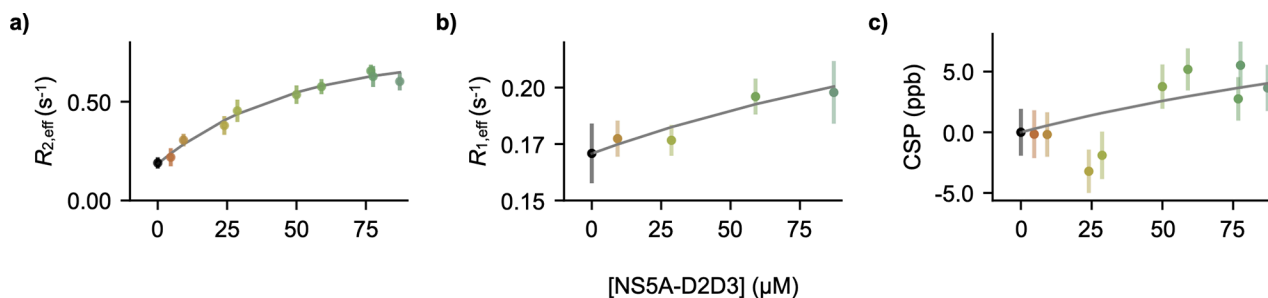


Figure 2. ^{19}F NMR reveals binding of a small molecule to a disordered protein. (a) $R_{2,\text{eff}}$ rates, obtained from Figure 1c as a function of NSSA-D2D3 concentration. Error bars represent the uncertainty in the $R_{2,\text{eff}}$ -fitted parameter from Figure 1c (from the covariance matrix). (b) $R_{1,\text{eff}}$ relaxation rates of 5-fluoroindole measured using the ^{19}F inversion recovery experiment² in the absence and presence of various concentrations of NSSA-D2D3. Error bars represent the uncertainty in the $R_{1,\text{eff}}$ -fitted parameter (from the covariance matrix of the exponential fit to intensities from the inversion recovery experiment). (c) Quantification of ligand-detected ^{19}F chemical shift perturbations relative to $50\ \mu\text{M}$ 5-fluoroindole alone (Figure S1c), measured in parts per billion. Error bars represent SEM from ≥ 2 technical replicates. A one-site binding model (gray curve), accounting for $R_{2,\text{eff}}$ rates, $R_{1,\text{eff}}$ rates, chemical shifts, and translational diffusion (see text), was fit to the data, yielding an affinity constant (K_{d}) of $260 \pm 110\ \mu\text{M}$.

S2). Fits obtained using all data are shown in Figures 2 and 3. The analysis gave a K_d of $260 \pm 110 \mu\text{M}$ (Figure 3a,b), a k_{off} of $800 \pm 500 \text{ s}^{-1}$ (Figure 3a,c), a $\tau_{c,F}$ of $27.0 \pm 1.3 \text{ ps}$, a $\tau_{c,B}$ of $46 \pm 10 \text{ ps}$ (Figure 3b,c), and a D_B of $(1.5 \pm 0.6) \times 10^{-9} \text{ m}^2 \text{ s}^{-1}$.

The rotational correlation time of the bound state of the small molecule ($\tau_{c,B}$) of 46 ps suggests that the small molecule

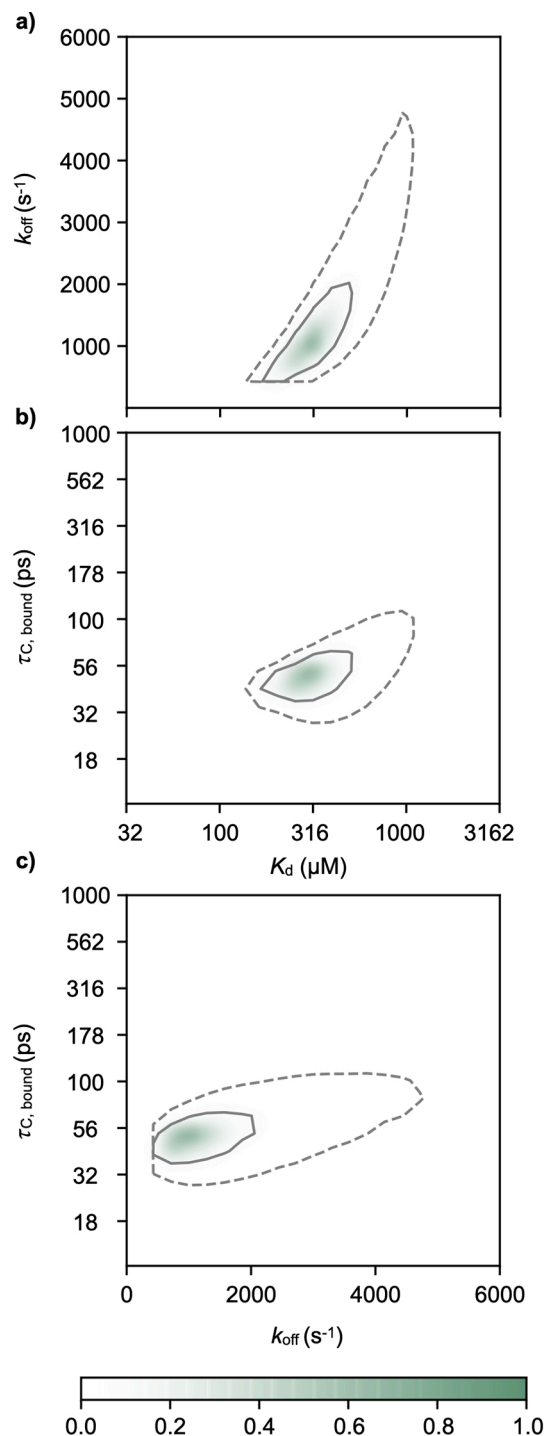


Figure 3. Normalized probability surfaces as functions of K_d , $\tau_{c,B}$, and k_{off} showing a micromolar binding affinity and fast dynamics in the bound state. The surfaces shown are calculated as $p(x,y) = \exp(-\chi^2 - \chi_{\text{min}}^2)/2$, where χ^2 is obtained from the least-squares fit of a one-site binding model to the experimental data. Solid and dashed lines represent the 68% and 95% confidence intervals, respectively.

is extremely dynamic within the bound state. This is particularly evident when considered in the context of the rotational correlation time of typical disordered proteins. Tryptophan residues, which, like 5-fluoroindole, also contain an indole motif, within disordered protein sequences have been reported to have fast rotational correlation components between approximately 100 and 260 ps, with longer components on the low nanoseconds time scale.³⁵ In this context, the $\tau_{c,B}$ that we observe, faster than the rotational correlation time of tryptophan residues in disordered proteins, suggests that the small molecule remains highly dynamic in the bound state. This extreme dynamics of the small molecule in the bound state is consistent with predictions of other small molecules interacting with IDPs.^{6,9,15}

This analysis allows not only for a sensitive detection of small-molecule binding to IDPs but also the quantification of the associated dynamics of the interaction, dissociation constant, and off-rates. The value of the derived K_d is particularly of note, since the micromolar interaction observed here is the same order as often observed for lead compounds in initial drug-screening programs.¹¹

To better understand the role of specificity in this interaction, we compared $R_{2,\text{eff}}$ measurements of 5-fluoroindole for samples containing similar densities of either PEG-20k or 75 μM NSSA-D2D3, given that the two polymers have roughly the same molecular weight. The decrease in the relaxation profile is more significant for NSSA-D2D3 than for PEG-20k (Figure S3), suggesting that the interaction between the IDP and 5-fluoroindole is distinct from simple crowding.

It has previously been reported that, at high concentrations, both NSSA-D2 and NSSA-D3 form transient secondary structures, potentially due to the formation of multimers.²⁴ To confirm that this also occurs for NSSA-D2D3, we performed circular dichroism (CD) measurements and observed a concentration-dependent loss of disorder at and above 100 μM , suggesting transient secondary structure formation (Figures S4 and S5). From the CD experiments a saturation of the more structured state could not be achieved, and therefore an equilibrium constant could not be determined for the multimerization.

Knowing that 5-fluoroindole interacts with NSSA-D2D3, we wondered whether this interaction alters the equilibrium of NSSA-D2D3 related to a change in the secondary structure propensity. At NSSA-D2D3 concentrations at or below 75 μM , we observed minimal changes in the presence of 50 μM 5-fluoroindole (Figure S5a,b), consistent with the protein-detected NMR experiments (Figures S6–S8, discussed below); that is, 5-fluoroindole generally does not alter the secondary structure propensity of NSSA-D2D3. At 200 μM NSSA-D2D3, very subtle changes were observed, suggesting that 5-fluoroindole may stabilize the less disordered state adopted by NSSA-D2D3 when the protein is at higher concentrations (Figure S5c). Of particular interest is that the NSSA-D2D3 system at high concentrations provides a way to assess the binding of 5-fluoroindole to a less disordered state. Notably, when chemical shift perturbations of 5-fluoroindole were measured in the presence of 200 μM NSSA-D2D3, larger chemical shift perturbations for both ^1H (Figure S4b) and ^{19}F (Figure S4c) were detected as compared to those detected for NSSA-D2D3 in its more dilute (and thus more disordered) state. This observation coincided with an increase in ^{19}F longitudinal ($R_{1,\text{eff}}$) and transverse ($R_{2,\text{eff}}$) relaxation rates of 0.24 ± 0.02 and $1.40 \pm 0.11 \text{ s}^{-1}$, respectively. These data

suggest a further increase in the effective correlation time of 5-fluoroindole when it interacts with the less disordered state of NSSA-D2D3.

NMR chemical shift perturbations are the gold-standard technique for screening and characterizing small-molecule binding to structured proteins. While significant protein-detected chemical shift perturbations have been reported for small-molecule interactions with IDPs,^{9–11} these are often small—a fraction of the peak line widths—or nearly undetectable in cases like the one presented here (Figures S6–S8). The largest protein-detected chemical shift perturbations we observe (more than 1 SD across all residues, each less than 12 ppb), which are consistent across two concentrations of 5-fluoroindole, occur at residues A308, W312, A313, T334, S414, and S448. Furthermore, it has recently been reported that heteronuclear single-quantum coherence spectra (HSQCs) of disordered proteins are highly prone to false-positive characterization of ligand interactions due to artifacts arising from mismatched pH.³⁶ In contrast, we report here that ligand-detected ¹⁹F transverse relaxation measurements are sensitive to small-molecule/IDP binding.

In this case study, we uncovered a micromolar binding affinity between 5-fluoroindole and NSSA-D2D3 in its disordered form, where chemical shift perturbations were minimal. We observe that transverse relaxation (R_2) is more sensitive to binding than either longitudinal relaxation (R_1) or chemical shift perturbations alone. In the 1D experiments, subtle changes can indeed be observed, but these could have easily been mistaken for mismatched buffers. These include very subtle increases in peak intensities, which can be explained by increases in longitudinal relaxation suggested by our model, combined with short relaxation delays (¹H: $D_1 = 1$ s, ¹⁹F: $D_1 = 0.5$ s). We also observe subtle chemical shift perturbations in the 1D experiments. The change in chemical shift upon binding leads to a chemical-exchange contribution to the transverse relaxation but not to longitudinal relaxation, making changes upon binding easier to detect via R_2 -based methods as compared to R_1 -based experiments. We do not observe line broadening in the 1D experiments, as they are overshadowed by ¹H–¹⁹F scalar couplings. Our integrative analysis, combining transverse and longitudinal relaxation, chemical shifts, and diffusion measurements, suggests that the small molecule remains very dynamic when interacting with NSSA-D2D3 in its disordered state. Our analysis of the NMR data coarsely assumes a singly averaged bound state, whereas MD simulations can frequently resolve multiple conformations within the bound ensemble.^{6,7,9,37} Additional types of NMR measurements could potentially provide further insight into the bound state ensemble.³⁸

We anticipate that ¹⁹F ligand-detected spin-relaxation experiments offer a promising route to characterize the conformational dynamics of small molecules bound to IDPs. Furthermore, this approach could be adapted as a medium-throughput screening strategy to identify small molecules that bind IDPs and other dynamic biomolecules, especially in cases where such interactions may be largely undetectable by other approaches. Using this tool, it is feasible to quantify the binding of numerous small-molecule/IDP interactions, including point mutants. This could facilitate the exploration of crucial inquiries regarding specificity and the nature of these dynamic interactions, ultimately contributing valuable insights into the prospective “drugability” of these dynamic biomolecules.

■ ASSOCIATED CONTENT

Data Availability Statement

Code that supports the findings of this study is available from GitHub at https://github.com/hansenlab-ucl/R2_IDP_small_mol. All data files are available from Zenodo at <https://zenodo.org/record/7892349#.ZFKHGC8w3Uo>.

Supporting Information

The Supporting Information is available free of charge at <https://pubs.acs.org/doi/10.1021/jacs.3c11614>.

Materials, methods, ligand-detected NMR chemical shifts in the absence and presence of protein, ¹H DOSY decays, transverse ¹⁹F relaxation curves of the small molecule in the absence and presence of a crowding agent, circular dichroism data of the protein at various concentrations in the presence and absence of the small molecule, and ¹H–¹⁵N HSQC spectra of the protein in the presence and absence of the small molecule (PDF)

■ AUTHOR INFORMATION

Corresponding Author

D. Flemming Hansen – Department of Structural and Molecular Biology, Division of Biosciences, University College London, London WC1E 6BT, U.K.; orcid.org/0000-0003-0891-220X; Email: d.hansen@ucl.ac.uk

Authors

Gabriella T. Heller – Department of Structural and Molecular Biology, Division of Biosciences, University College London, London WC1E 6BT, U.K.; orcid.org/0000-0002-5672-0467

Vaibhav Kumar Shukla – Department of Structural and Molecular Biology, Division of Biosciences, University College London, London WC1E 6BT, U.K.

Angelo Miguel Figueiredo – Department of Structural and Molecular Biology, Division of Biosciences, University College London, London WC1E 6BT, U.K.; orcid.org/0000-0001-7039-5341

Complete contact information is available at: <https://pubs.acs.org/10.1021/jacs.3c11614>

Author Contributions

G.T.H. and V.K.S. produced samples of NSSA-D2D3. G.T.H., A.M.F., and D.F.H. collected and analyzed the data. All authors discussed the results and commented on the paper. All authors have given approval to the final version of the manuscript.

Funding

G.T.H. was supported by Schmidt Science Fellows, Rosalind Franklin Research Fellowship from Newnham College, Cambridge, and a BBSRC Discovery Fellowship (BB/X009955/1). This work was also supported by the UCL Wellcome Institutional Strategic Support Fund (204841/Z/16/Z). The BBSRC (BB/R000255/1), Wellcome Trust (ref101569/z/13/z), and the EPSRC are acknowledged for supporting the NMR facility at University College London. Access to ultra-high field NMR spectrometers was supported by the Francis Crick Institute through provision of access to the MRC Biomedical NMR Centre. The Francis Crick Institute receives its core funding from Cancer Research UK (FC001029), the UK Medical Research Council (FC001029), and the Wellcome Trust (FC001029). D.F.H. is supported by the UKRI and EPSRC (EP/X036782/1).

Notes

The authors declare no competing financial interest.

ACKNOWLEDGMENTS

The authors acknowledge Gogulan Karunanithy and Geoff Kelly for helpful discussion. For the purpose of open access, the authors have applied a Creative Commons Attribution (CC BY) licence to any Author Accepted Manuscript version arising. The authors also acknowledge Khushboo Matwani for assistance with protein production.

ABBREVIATIONS

CD, circular dichroism; CPMG, Carr–Purcell–Meiboom–Gill; IDP, intrinsically disordered protein; MD, molecular dynamics; NMR, nuclear magnetic resonance; NSSA-D2D3, disordered domains 2 and 3 of the non-structural protein 5A

REFERENCES

- (1) Overbeck, J. H.; Kremer, W.; Sprangers, R. A suite of ^{19}F based relaxation dispersion experiments to assess biomolecular motions. *J. Biomol. NMR* **2020**, *74* (12), 753–766.
- (2) Vold, R. L. On the measurement of transverse relaxation rates in complex spin systems. *J. Chem. Phys.* **1972**, *56* (7), 3210–3216.
- (3) Dyson, H. J.; Wright, P. E. Intrinsically unstructured proteins and their functions. *Nat. Rev. Mol. Cell Biol.* **2005**, *6* (3), 197–208.
- (4) Cszizmok, V.; Follis, A. V.; Kriwacki, R. W.; Forman-Kay, J. D. Dynamic protein interaction networks and new structural paradigms in signaling. *Chem. Rev.* **2016**, *116* (11), 6424–6462.
- (5) Tompa, P. Intrinsically unstructured proteins. *Trends Biochem. Sci.* **2002**, *27* (10), 527–533.
- (6) Heller, G. T.; Aprile, F. A.; Michaels, T. C.; Limbocker, R.; Perni, M.; Ruggeri, F. S.; Mannini, B.; Löhr, T.; Bonomi, M.; Camilloni, C.; et al. Small-molecule sequestration of amyloid- β as a drug discovery strategy for Alzheimer's disease. *Sci. Adv.* **2020**, *6* (45), No. eabb5924.
- (7) Heller, G. T.; Aprile, F. A.; Bonomi, M.; Camilloni, C.; De Simone, A.; Vendruscolo, M. Sequence specificity in the entropy-driven binding of a small molecule and a disordered peptide. *J. Mol. Biol.* **2017**, *429* (18), 2772–2779.
- (8) Follis, A. V.; Hammoudeh, D. I.; Wang, H.; Prochownik, E. V.; Metallo, S. J. Structural rationale for the coupled binding and unfolding of the c-Myc oncoprotein by small molecules. *Chem. Biol.* **2008**, *15* (11), 1149–1155.
- (9) Robustelli, P.; Ibanez-de-Opakua, A.; Campbell-Bezaz, C.; Giordanetto, F.; Becker, S.; Zweckstetter, M.; Pan, A. C.; Shaw, D. E. Molecular basis of small-molecule binding to α -synuclein. *J. Am. Chem. Soc.* **2022**, *144* (6), 2501–2510.
- (10) Basu, S.; Martinez-Cristobal, P.; Pesarrodona, M.; Frigolé-Vivas, M.; Lewis, M.; Szulc, E.; Bañuelos, C. A.; Sánchez-Zarzalejo, C.; Bielskutė, S.; Zhu, J.; et al. Rational optimization of a transcription factor activation domain inhibitor. *Nat. Struct. Mol. Biol.* **2023**, *30*, 1958–1969.
- (11) Iconaru, L. I.; Ban, D.; Bharatham, K.; Ramanathan, A.; Zhang, W.; Shelat, A. A.; Zuo, J.; Kriwacki, R. W. Discovery of small molecules that inhibit the disordered protein, p27Kip1. *Sci. Rep.* **2015**, *5* (1), 15686.
- (12) Ban, D.; Iconaru, L. I.; Ramanathan, A.; Zuo, J.; Kriwacki, R. W. A small molecule causes a population shift in the conformational landscape of an intrinsically disordered protein. *J. Am. Chem. Soc.* **2017**, *139* (39), 13692–13700.
- (13) Heller, G. T.; Sormanni, P.; Vendruscolo, M. Targeting disordered proteins with small molecules using entropy. *Trends Biochem. Sci.* **2015**, *40* (9), 491–496.
- (14) Jin, F.; Yu, C.; Lai, L.; Liu, Z. Ligand clouds around protein clouds: a scenario of ligand binding with intrinsically disordered proteins. *PLoS Computat. Biol.* **2013**, *9* (10), No. e1003249.
- (15) Löhr, T.; Kohlhoff, K.; Heller, G. T.; Camilloni, C.; Vendruscolo, M. A small molecule stabilizes the disordered native state of the Alzheimer's A β peptide. *ACS Chem. Neurosci.* **2022**, *13* (12), 1738–1745.
- (16) Thomasen, F. E.; Lindorff-Larsen, K. Conformational ensembles of intrinsically disordered proteins and flexible multi-domain proteins. *Biochem. Soc. Trans.* **2022**, *50* (1), 541–554.
- (17) Rauscher, S.; Gapsys, V.; Gajda, M. J.; Zweckstetter, M.; De Groot, B. L.; Grubmüller, H. Structural ensembles of intrinsically disordered proteins depend strongly on force field: a comparison to experiment. *J. Chem. Theory Comput.* **2015**, *11* (11), 5513–5524.
- (18) Bonomi, M.; Heller, G. T.; Camilloni, C.; Vendruscolo, M. Principles of protein structural ensemble determination. *Curr. Opin. Struct. Biol.* **2017**, *42*, 106–116.
- (19) Bottaro, S.; Lindorff-Larsen, K. Biophysical experiments and biomolecular simulations: A perfect match? *Science* **2018**, *361* (6400), 355–360.
- (20) Heller, G.; Yu, L.; Hansen, D. Characterising intrinsically disordered proteins using NMR spectroscopy and MD simulations. *NMR Spectroscopy for Probing Functional Dynamics at Biological Interfaces*; Royal Society of Chemistry, 2022; pp 383–410.
- (21) Felli, I. C.; Pierattelli, R. *Intrinsically disordered proteins studied by NMR spectroscopy*; Springer, 2015.
- (22) Shukla, V. K.; Heller, G. T.; Hansen, D. F. Biomolecular NMR spectroscopy in the era of artificial intelligence. *Structure* **2023**, *31* (11), 1360–1374.
- (23) Williamson, M. P. Using chemical shift perturbation to characterise ligand binding. *Prog. Nucl. Magn. Reson. Spectrosc.* **2013**, *73*, 1–16.
- (24) Badillo, A.; Receveur-Brechot, V.; Sarrazin, S.; Cantrelle, F.-X.; Delolme, F.; Fogeron, M.-L.; Molle, J.; Montserret, R.; Bockmann, A.; Bartschlag, R.; et al. Overall structural model of NSSA protein from hepatitis C virus and modulation by mutations conferring resistance of virus replication to cyclosporin A. *Biochemistry* **2017**, *56* (24), 3029–3048.
- (25) Dujardin, M.; Madan, V.; Montserret, R.; Ahuja, P.; Huvent, I.; Launay, H.; Leroy, A.; Bartschlag, R.; Penin, F.; Lippens, G.; Hanouille, X. A proline-tryptophan turn in the intrinsically disordered domain 2 of NSSA protein is essential for hepatitis C virus RNA replication. *J. Biol. Chem.* **2015**, *290* (31), 19104–19120.
- (26) Hanouille, X.; Badillo, A.; Wieruszkeski, J.-M.; Verdegem, D.; Landrieu, I.; Bartschlag, R.; Penin, F.; Lippens, G. Hepatitis C virus NSSA protein is a substrate for the peptidyl-prolyl cis/trans isomerase activity of cyclophilins A and B. *J. Biol. Chem.* **2009**, *284* (20), 13589–13601.
- (27) Meiboom, S.; Gill, D. Modified spin-echo method for measuring nuclear relaxation times. *Rev. Sci. Instrum.* **1958**, *29* (8), 688–691.
- (28) Carr, H. Y.; Purcell, E. M. Effects of diffusion on free precession in nuclear magnetic resonance experiments. *Phys. Rev.* **1954**, *94* (3), 630.
- (29) Gerathanassis, I. Methods of avoiding the effects of acoustic ringing in pulsed Fourier transform nuclear magnetic resonance spectroscopy. *Prog. Nucl. Magn. Reson. Spectrosc.* **1987**, *19* (3), 267–329.
- (30) McConnell, H. M. Reaction rates by nuclear magnetic resonance. *J. Chem. Phys.* **1958**, *28* (3), 430–431.
- (31) Kroenke, C. D.; Loria, J. P.; Lee, L. K.; Rance, M.; Palmer, A. G. Longitudinal and transverse ^1H - ^{15}N dipolar/ ^{15}N chemical shift anisotropy relaxation interference: unambiguous determination of rotational diffusion tensors and chemical exchange effects in biological macromolecules. *J. Am. Chem. Soc.* **1998**, *120* (31), 7905–7915.
- (32) Abragam, A. *The principles of nuclear magnetism*; Oxford University Press, 1961.
- (33) Lu, M.; Ishima, R.; Polenova, T.; Gronenborn, A. M. ^{19}F NMR relaxation studies of fluorosubstituted tryptophans. *J. Biomol. NMR* **2019**, *73* (8), 401–409.
- (34) Lu, M.; Sarkar, S.; Wang, M.; Kraus, J.; Fritz, M.; Quinn, C. M.; Bai, S.; Holmes, S. T.; Dybowski, C.; Yap, G. P.; et al. ^{19}F magic angle

spinning NMR spectroscopy and density functional theory calculations of fluorosubstituted tryptophans: integrating experiment and theory for accurate determination of chemical shift tensors. *J. Phys. Chem. B* **2018**, *122* (23), 6148–6155.

(35) Jain, N.; Narang, D.; Bhasne, K.; Dalal, V.; Arya, S.; Bhattacharya, M.; Mukhopadhyay, S. Direct observation of the intrinsic backbone torsional mobility of disordered proteins. *Biophys. J.* **2016**, *111* (4), 768–774.

(36) Pandey, A. K.; Buchholz, C. R.; Nathan Kochen, N.; Pomerantz, W. C.; Braun, A. R.; Sachs, J. N. pH effects can dominate chemical shift perturbations in ^1H , ^{15}N -HSQC NMR spectroscopy for studies of small molecule/ α -synuclein interactions. *ACS Chem. Neurosci.* **2023**, *14* (4), 800–808.

(37) Zhu, J.; Salvatella, X.; Robustelli, P. Small molecules targeting the disordered transactivation domain of the androgen receptor induce the formation of collapsed helical states. *Nat. Commun.* **2022**, *13* (1), 6390.

(38) Tiwari, V. P.; Toyama, Y.; De, D.; Kay, L. E.; Vallurupalli, P. The A39G FF domain folds on a volcano-shaped free energy surface via separate pathways. *Proc. Natl. Acad. Sci. U. S. A.* **2021**, *118* (46), No. e2115113118.